2023 IEEE International Conference on Robotics and Automation (ICRA 2023)
May 29 - June 2, 2023. London, UK

Passive robotic gripper using a contact-based locking mechanism

Issei Nate[1], Zhongkui Wang[2], and Shinichi Hirai[1]

Abstract— **Robotic end-effectors have been developed for various applications. Most of them are driven by electric or pneumatic actuator/actuators, which usually make the end-effector bulky and vulnerable due to the external cables and air tubes. In this study, we propose a novel passive robotic gripper with a locking mechanism that does not require any actuators. Locking and unlocking of the gripper fingers are performed through contact with external environment, such as ground, table, and conveyor. To facilitate gripper design, modeling of the deformed finger shape was conducted, and experimental validation was performed. A robotic gripper with eight such passive fingers were fabricated using 3D printer. Experiments were conducted to investigate the grasping capacities in terms of object size and weight. We found that the larger the object, the greater the weight capacity of the gripper, which increased significantly when the object exceeded a certain size. In addition, experiments on grasping various food products were carried out and results suggested that the proposed gripper could grasp objects with complex shapes and soft fragile properties, but damages were caused on very fragile objects due to the rigid structure of the gripper.**

I. INTRODUCTION

Robotic gripper or hand, as one of the robotic end-effectors, has always been an important research field because it is the key component that makes direct contact with the target object or environment to complete an actual task. As a result, a wide variety of robot grippers have been developed as robots have become more popular in recent years [1], [2], [3], [4]. There are many principles for actuating robotic grippers, for example using electric motor and pneumatic system [5], [6], [7].

Motors are often used as the actuating principle of general grippers [8]. Motor has advantages of generating strong grasping force and being able to achieve precise control of rotation angle. Therefore, it is possible to adjust the opening and closing of the gripper based on the application and weight of the target object. However, motor-driven grippers have the disadvantages of being bulky and having difficulties to be used in underwater applications, such as underwater exploration and automation in the fishery industry [9], [10]. Because a robot arm has a weight capacity, the maximum load of the object that the robot can carry is correspondingly reduced if the gripper is heavy. For flying robots, such as drones, the overall weight should be as light as possible, so heavy grippers can be a fatal drawback [11], [12].

[1]I. Nate and S. Hirai are with Soft Robotics Laboratory, Department of Robotics, Ritsumeikan University, Noji-Higashi 1-1-1, Kusatsu, 525-8577 Shiga, Japan. rr0111rv@ed.ritsumei.ac.jp, hirai@se.ritsumei.ac.jp

[2]Z. Wang is with Cloud Robotics Laboratory, Department of Robotics, Ritsumeikan University, Noji-Higashi 1-1-1, Kusatsu, 525-8577 Shiga, Japan. wangzk@fc.ritsumei.ac.jp

(a) (b)

Fig. 1: Proposed passive finger with locking mechanism (a) and the eight-fingered robotic gripper (b).

In the food industry, pneumatically driven grippers are preferred to prevent contamination [13], [14]. Pneumatically driven grippers are also suitable for grasping soft and fragile objects. However, pneumatic actuators usually require a pneumatic system including air compressor, pressure regulator, and solenoid valves, to generate and control desired pressure. Although pneumatic system can be installed away from the gripper and keep the gripper compact, it still occupies space, generates noise, and adds extra cost to the entire robotic system. In addition, air tubes and connectors are needed to connect the pneumatic system and the gripper. These connections often cause operational issues, such air leakage, pressure loss, and piping trouble.

To remove actuators, researchers have been working on various passive robotic end-effectors and self-locking mechanisms. Zhao *et al.* proposed a passive mechanism based on suction cup for perching flying robots onto objects [15]. Qi *et al.* developed a passive bistable soft gripper inspired by sea-anemone and the grasping (locking) is realized by pressing the gripper onto the target object [16]. However, unlocking motion requires air pressure input. Similarly, a gecko-inspired soft passive gripper was proposed by Seibel *et al.* using a commercial tape with mushroom-shaped adhesive structures to passively grasp flat objects [17]. The gripper also needs air pressure input for releasing the grasped object. A passive spine gripper was proposed for free-climbing robot in extreme terrain [18]. The fine spine of the gripper enables it to passively and adaptively latch onto the microscopic asperities of rough surface, but it requires a motor to release the gripper. In addition, a passive gripper inspired by Manduca sexta and the Fin Ray® Effect was proposed by Crooks *et al.* and the gripper requires power to open and close but not

to maintain a grasp [2]. For self-locking mechanism, Guo *et al.* developed a self-locking mechanism realized by a rigid ratchet-and-pawl structure to enhance the stiffness of a pneumatic soft gripper [19]. The locking process is automatically realized by the bending of the pneumatic gripper and the unlocking process is triggered by a pneumatic actuator. Li *et al.* developed a soft robotic gripper with passive particle jamming and the gripper stiffness can be controlled by the air pressure applied to gripper [20]. The particle jamming can be considered as self-locking among particles through friction. In addition, Hsu *et al.* proposed self-locking underactuated gripper for the purpose of mounting on a humanoid robot to achieve firm and robust grasp [21]. The self-locking was realized by a drum brake actuated by a differential gear.

In this paper, we propose a novel passive gripper with finger-locking mechanism, as shown in Fig. 1. Both locking and unlocking of the fingers were realized through contact with the environment, such as ground, table, and conveyor. It does not require any actuators to trigger or control the locking and unlocking. As a result, it also does not need any cables or air tubes, and this makes the robotic gripper compact and low cost. The design and working principle of the gripper are explained in Section II. To facilitate gripper design, a computational model of the deformed finger is formulated and experimentally validated in Section III. In Section IV, the weight capacity of the gripper is characterized and the experimental results on grasping various food products were discussed. Finally, Section V conclude the paper with suggestions of future work.

II. Gripper Design

A. Gripper Features

The gripper developed in this study is a multi-fingered and multi-joint gripper, as shown in Fig. 1. Each finger consisted of three parts as shown in Figs. 2a, 2b, and 2c, respectively. The dimensions of the parts are given in Fig. 2d. The thin plate shown in Fig. 2c passes through the inside of the finger and the top side of the plate is fixed to the base of the finger. The parts were fabricated using a 3D printer (Prusa, i3 MK3, Prusa Research) [22]. Since the plate works as a flat spring for opening the fingers, it is desirable that the plate is made of a material that is resistant to plastic deformation. In our experiments, we tried two materials of PETG and PLA, which are often used by 3D printing. We finally choose PETG to fabricate the plate because PETG had better performance than PLA. By assembling multiple middle parts, one tip part, and one plate, we obtain a finger as shown in Fig. 1a.

When the gripper is pressed against the ground, the finger bends and the plate moves forward relatively because of the difference in the curvature radius between the finger joint and the plate, as shown in Fig. 3. This relationship achieves the locking and unlocking functions. Moreover, the gripper has the following two advantages. First, it is unnecessary to pay attention to contact with the ground. Conventional grippers are at risk of being damaged by contact with the ground [23]; however, the proposed gripper eliminates this risk. The second is the ability to slide the finger under the object when grabbing it [24], [25]. Therefore, the gripper can grasp objects from their bottom, and as a result, it can be used to grasp soft and fragile objects.

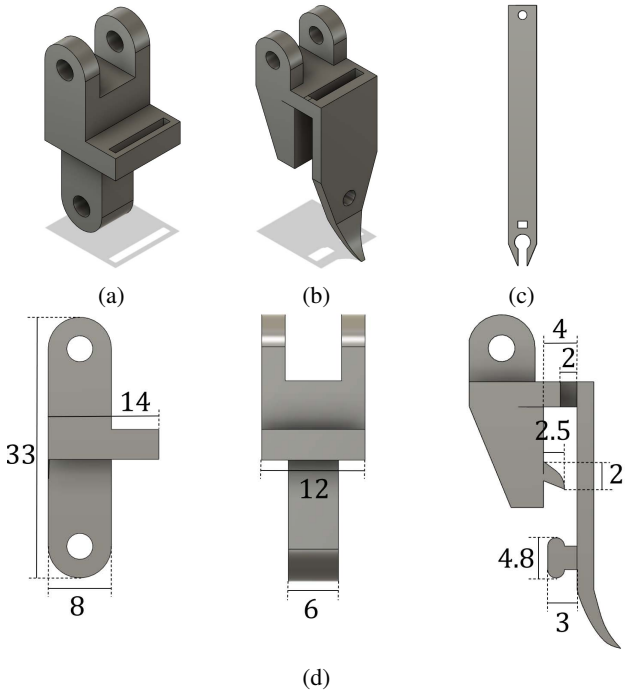

Fig. 2: Finger Components of (a) middle part, (b) tip part, (c) thin plate, and (d) the dimensions of the middle and tip parts.

B. Locking Principle

The locking mechanism on each finger works through contact between the plate and fingertip. There are two types of protrusion on the fingertip part, as shown in Fig. 2d. Figs. 4a, 4b, 4c show the locking principle. When the gripper is pressed against the ground, the finger receives force from the ground and bends inward, as shown in Fig. 4a. At this state, the upper protrusion overlaps with the circular hole in the plate, and it does not make contact with the plate. Therefore, the tip of the plate is located outside the lower

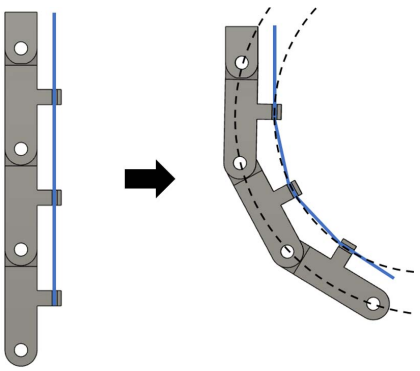

Fig. 3: Curvature difference between the joints and the plate.

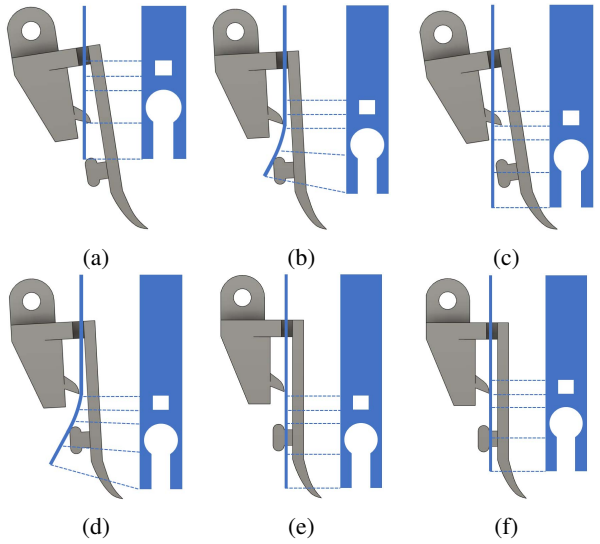

Fig. 4: Principle of locking in (a), (b), (c) and unlocking in (d), (e), (f).

protrusion. Fig. 4b shows the state in which the gripper is further pressed, and the plate moves forward. At this state, the upper protrusion contacts the plate. The plate bends and rides on the lower protrusion because the plate and lower protrusion are positioned as shown in Fig. 4b. When the finger is further pressed as shown in Fig. 4c, the upper protrusion fits into the square hole of the plate and the locking is triggered. Because the plate does not retract in the locking state, the finger becomes relatively rigid and therefore can carry large weight or external load.

C. Unlocking Principle

The principle of unlocking is illustrated in Figs. 4d, 4e, and 4f. In the locking state, the plate cannot move backward because of the shape of the upper protrusion, but it can move forward. Fig. 4d shows the state in which the gripper is further pressed from the locking state and the plate moves forward. At this state, the upper protrusion contacts the plate again, and the plate receives a force from the upper protrusion. At the state shown in Fig. 4e, the plate is slightly advanced from the state shown in Fig. 4d. This is the lowest point in the mechanism. In this state, the lower protrusion overlaps with the circular hole in the plate. The plate fits into the lower protrusion because it receives a force from the upper protrusion. Subsequently, the gripper is raised. Fig. 4f shows the state in which the plate is restored, and the upper protrusion overlaps with the square hole of the plate. In this state, the tip of the plate is located at the right side of the lower protrusion; therefore, the upper protrusion does not fit into the square hole in the plate. As a result, the plate can be retracted without triggering the locking motion.

III. DEFORMED SHAPE MODELING

A. Geometrical Modeling

The closed gripper shape is determined by the position where the locking functions. Therefore, when we design the

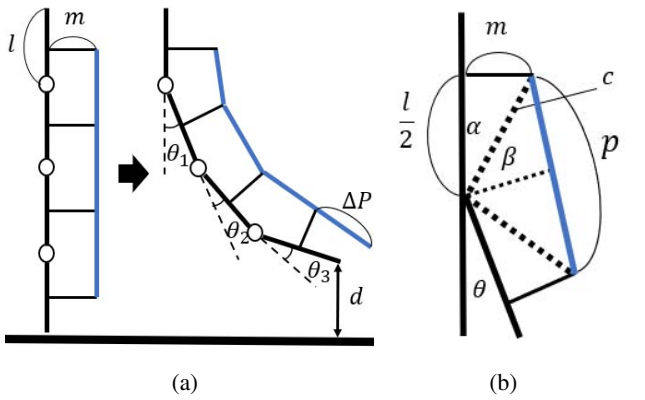

Fig. 5: Geometric relationship between the finger and plate (a) and a close-up view of one joint (b). Black lines denote the finger and blue lines indicate the thin plate.

gripper, it is necessary to clarify the relationship between the amount of pressing of the gripper and the extension of the plate. The positional relationship between the plate and the joint is shown in Fig. 5. The plate deforms continuously; however, for simplicity, it is assumed that the plate bends only at the finger guide (black lines connect the finger parts and the plate). Here, we define l, m, c, p, θ, α, and β as shown in Fig. 5b, and they can be calculated as

$$\alpha = \arctan\left(\frac{2m}{l}\right) \tag{1}$$

$$\beta = \frac{\pi-\theta}{2} - \alpha \tag{2}$$

$$c = \sqrt{\left(\frac{l}{2}\right)^2 + m^2} \tag{3}$$

$$p = 2c\sin\beta. \tag{4}$$

If the number of joints is n, the plate extension Δp can be simply determined as

$$\Delta p = n\,(l-p)\,. \tag{5}$$

In addition, let S be the horizontal displacement of the fingertip and it can be then calculated as

$$S = l\sum_{i=1}^{n}\sin\left(\sum_{j=1}^{i}\theta_j\right). \tag{6}$$

From the above, if the rotation angle of each joint is obtained, the amount of extension of the plate and the closing amount of the finger can be calculated accordingly.

B. Joint Angle Determination

Obtaining the rotation angle of each joint is described in this section. When the plate is bent, it deforms to a shape with the minimum elastic potential energy. In this research, as shown in Fig. 5a, it was assumed that the restoring force is proportional to the rotation angle acting on each joint. Here,

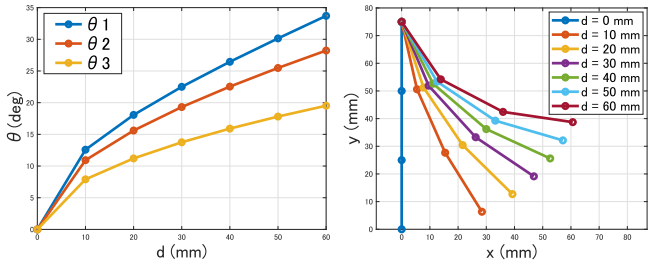

(a) (b)

Fig. 6: Simulation results of (a) rotation angle of each joint and (b) deformed shape of the finger with different pressing distances indicated by different colors.

let k be the spring modulus, and E be the energy stored in the deformed finger. Then, E can be calculated as

$$E = \frac{1}{2}\sum_{i=1}^{n} k\theta_i^2. \tag{7}$$

Let d be the pressed distance (Fig. 5a) after the fingertip touches the ground and it can be expressed as

$$d = nl - l\sum_{i=1}^{n}\cos\left(\sum_{j=1}^{i}\theta_j\right) \tag{8}$$

The deformed shape can be then determined by finding the joint angles θ_i that minimize the potential energy E under the condition of Eq. 8.

C. Simulation Results

The fabricated gripper has geometrical parameters of $l = 25\,\text{mm}$ and $n = 3$. Fig. 6a shows the calculation results of bending angle θ with different pressing distances d. Fig. 6b shows the simulation results of the deformed shape of the finger. These results reveal that the joint at the tip has a smaller rotation angle.

D. Experimental Validation

The actual rotation angle of each joint was measured to compare with the simulation results. The deformed state of the finger was captured using a camera, and the rotation angle of each joint was then calculated based on the pixel coordinates in the image. As shown in Fig. 7, six images were captured by pressing the finger with a distance interval of 10 mm from the state where the finger touches the ground. The locking was triggered at $d = 60\,\text{mm}$. Fig. 8a shows the comparison between the simulated and measured joint angles. In the range of $d < 40\,\text{mm}$, the measured and calculated angles differed significantly. However, in the range of $d \geq 40\,\text{mm}$, the difference was relatively small. This is because, when $d < 40\,\text{mm}$, an external force acted on the plate to prevent it from moving. The state in Fig. 4b corresponds to this behavior. Therefore, the model can predict the shape of the state when the locking is triggered but not before locking happens. However, when we design the gripper, the shape of locked finger is in main concern.

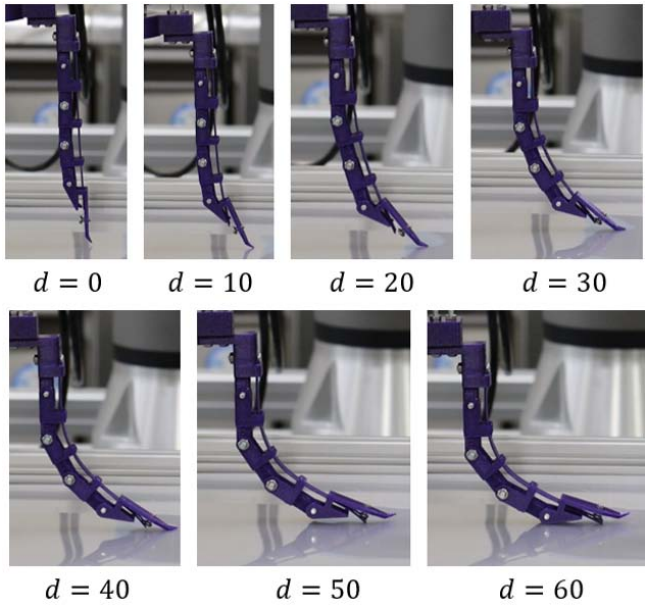

Fig. 7: Experimental snapshots of the deformed finger at different pressing distances from 0 mm to 60 mm.

Therefore, the proposed model can be used for facilitating the gripper design.

IV. GRASPING EXPERIMENTS

A. Experimental Setup

The gripper shown in Fig. 1b was fabricated to grasp various objects. The gripper consists of eight fingers arranged in a circular configuration and each finger has three joints. If the finger number is less than eight, the gap between neighboring fingers would be large for grasping small objects. Therefore, we decided on using eight fingers for our grasping experiments. The diameter of the circular shape formed by the fingers was designed as 120 mm, and objects smaller than this can be grasped. On the other hand, we designed the finger to generate a closing displacement of $S = 50\,\text{mm}$ on each finger. Therefore, a 20 mm gap remains theoretically when the gripper is closed. When $S = 50$, the combinations of θ that satisfy Eq. 7 are obtained as: $\theta_1 = 24.51\,\text{deg}$,

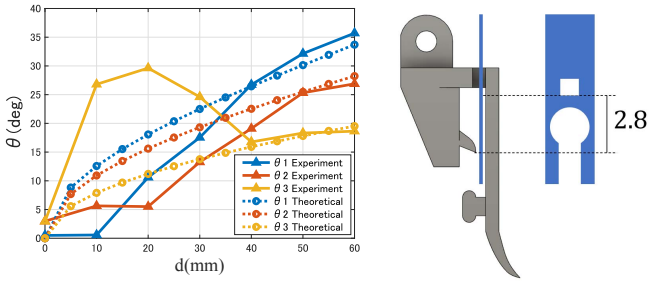

(a) (b)

Fig. 8: (a) Comparison of simulated and measured joint angles at different pressing distances. (b) Initial position of the plate derived from calculation results.

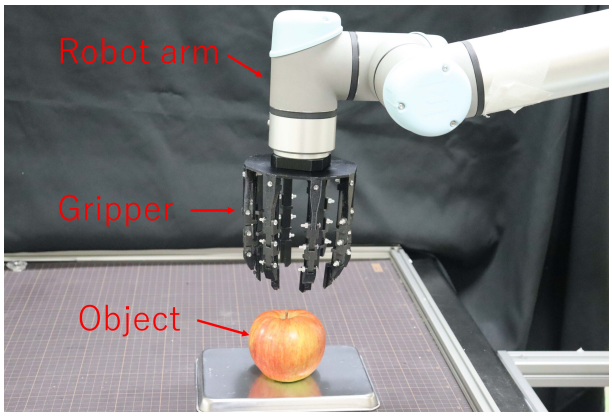

Fig. 9: Experimental setup for grasping tests.

$\theta_2 = 20.96$ deg, and $\theta_3 = 14.86$ deg, respectively. Therefore, as shown in Fig. 8b, the plate is fixed at the position where the square hole is 2.8 mm away from the protrusion in the initial state. The experimental setup is illustrated in Fig. 9. The gripper was attached to a robotic manipulator (UR5e, UNIVERSAL ROBOTS), and the gripper is opened and closed by moving the manipulator up and down. The object was placed on a stainless tray below the gripper.

B. Weight Grasping Tests

When a finger in the locked state receives a vertically downward load, the joint at the base of the finger is extended, and the joint at the tip is bent, as shown in Fig. 10a. This is because the finger deforms when the length of the plate is constant, while the finger is locked. Therefore, the tip opens slightly outward, owing to the weight of the object.

Experiments were conducted to investigate the relationship between the size and weight of objects that can be grasped. The experimental method is illustrated in Fig. 10b. Hemispheres with different diameters were fabricated using a 3D printer, and each of them was grasped by the gripper. Different dead weights were hung on the hemisphere for the tests and the weights were increased gradually until the gripper failed to grasp. Experimental results are plotted in Fig. 11. We can observe a small jump in between diameter of 40 mm and 50 mm. We believe that this small jump is caused by the deformation shown in Fig. 10a. The bending of the fingertip occurred when the diameter of the hemisphere was less than 50 mm, whereas the elastic deformation of the entire gripper starts when the diameter was greater than 50 mm. Therefore, for objects larger than 50 mm, the weight capacity is considered to be better for the current gripper.

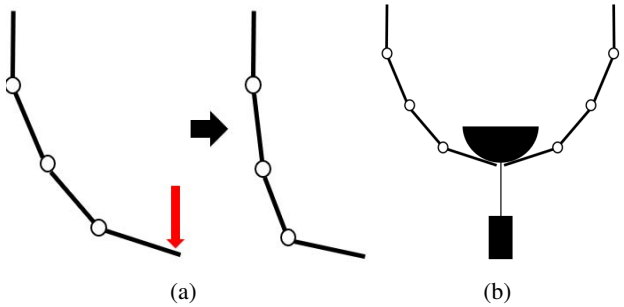

Fig. 10: Finger deformation due to load in (a) and the experimental method in (b) for weight test.

C. Food Grasping Tests

Grasping experiments were conducted using various food products (Table I) with different properties to evaluate the performance of the gripper. In the experiments, the food products were grasped and lifted, and then placed back to the same location. If the food product could be lifted and placed back without obvious damages, it is considered as success and indicated as a "◯" in Table I. If the food product could be lifted and placed back but with damages, it is denoted as a "△". On the other hand, if the food product could not be lifted, it is considered as a failure and indicated as a "×". The experimental results are listed in Table I and snapshots of the gripper holding the food products are shown in Fig. 12. Videos showing the grasping experiments can be found in the supplementary material, in which the gripper was also used to grasp a jellyfish from a water tank to demonstrate the ability of using the gripper for underwater tasks. An apple and a cherry tomato could be grasped, which shows that the proposed gripper can handle heavy and small objects. A mushroom and a tentacle were successfully grasped, demonstrating that objects with complex shapes can be grasped by the gripper. Soft and fragile objects with low friction could also be grasped, such as a Pollock roe and a pudding, but some damages were caused by the rigid structure of the gripper. To avoid damaging fragile objects, soft contact should be considered, and it will be one of our future work.

V. CONCLUSIONS

An actuator is usually required to develop a robotic gripper. Actuators are often heavy, bulky, and expensive. Cabling and piping are also troublesome and could be one of the reasons causing system failure. To solve this problem, a passive robotic gripper capable of self-locking and self-unlocking was proposed in this paper. The locking and unlocking of the gripper are realized by pressing the gripper

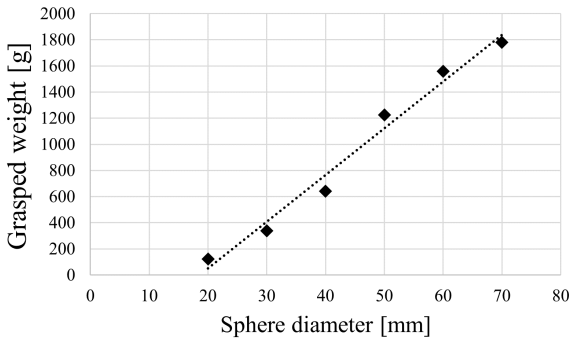

Fig. 11: Results of weight grasping tests

TABLE I: Food products used for the grasping tests and the test results.

Name	Apple	Cherry tomatoes	Mushroom	Pollock roe	tentacle	Pudding
Picture				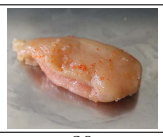		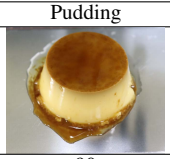
Weight (g)	361	12	22	39	83	90
Length (mm)	85	28	59	89	82	80
Result	◯	◯	◯	△	◯	△

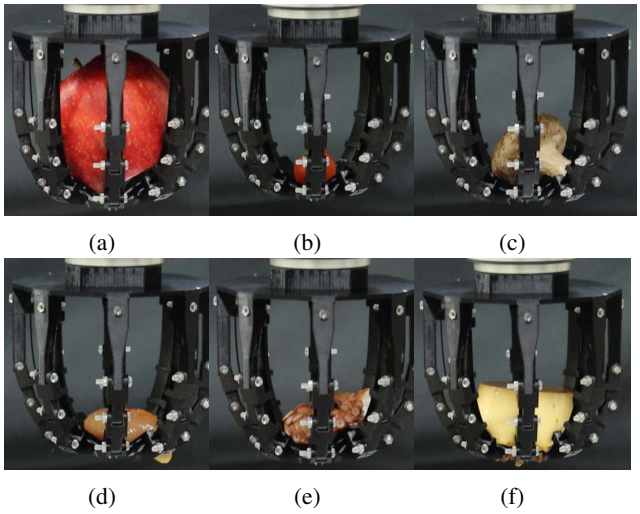

(a) (b) (c) (d) (e) (f)

Fig. 12: Holding food images of (a) apple, (b) cherry tomatoes, (c) mushroom, (d) fish eggs, (e) tentacle and (f) pudding.

against environment. A computational model was derived to calculate the deformed shape of the gripper finger. The model was validated through experiments, and we found that the model could well predict the deformed shape of the finger at the locking state and the model was used to facilitate the finger structure design. Two experiments were conducted using a 3D printed gripper with eight fingers. The weight grasping experiment showed that the maximum weight which can be grasped by the gripper depending on the size of the object. With a diameter of 70 mm, the gripper could grasp a weight of 1.8 kg. Grasping experiments on various food products revealed that the passive gripper is capable of handling large and heavy objects, and objects with complex geometry and low friction. For fragile objects, the current gripper can grasp and lift them, but the objects may be damaged by the rigid fingers.

The proposed gripper also has few limitations. The locking and unlocking can be only realized on flat surfaces with low friction. In addition, contact with the surface is required to be as vertical as possible to ensure a proper locking and unlocking motion. In future work, force characterization of the gripper will be conducted to further understand the capability of the gripper. Making the finger capable of grasping fragile objects will also be investigated in the future.

ACKNOWLEDGMENT

This work was supported by the Cabinet Office (CAO), Cross-Ministrial Strategic Innovation Promotion Program (SIP), and an intelligent knowledge processing infrastructure that integrates physical and virtual domains (funding agency: NEDO), and in part by JSPS KAKENHI Grant Number 20K04406.

REFERENCES

[1] Y. Makiyama, Z. Wang, and S. Hirai, “A pneumatic needle gripper for handling shredded food products”, 2020 IEEE International Conference on Real-time Computing and Robotics (RCAR), pp. 183-187, Sept., 2020.

[2] W. Crooks, S. Rozen-Levy, B. Trimmer, C. Rogers, W. Messner, “Passive gripper inspired by Manduca sexta and the Fin Ray® Effect”, International Journal of Advanced Robotic Systems, vol. 14, no. 4, 2017.

[3] Z. Wang, R. Kanegae, and S. Hirai, “Circular shell gripper for handling food products”, Soft robotics, vol. 8, no. 5, pp. 542-554, 2021.

[4] J. Amend, N. Cheng, S. Fakhouri, and B. Culley, “Soft robotics commercialization: Jamming grippers from research to product”, Soft robotics, vol. 3, no. 4, pp. 213-222, 2016.

[5] C. M. Lin, and C. F. Hsu, “Adaptive fuzzy sliding-mode control for induction servomotor systems”, IEEE Transactions on Energy Conversion, vol. 19, no. 2, pp. 362-368, 2004.

[6] J. L. Shearer, “Study of pneumatic processes in the continuous control of motion with compressed air—I”, Transactions of the American Society of Mechanical Engineers, vol. 78, no. 2, pp. 233-241, 1956.

[7] Y. Shen, H. Osumi, and T. Arai, “Set of manipulating forces in wire driven systems”, IEEE/RSJ International Conference on Intelligent Robots and Systems (IROS’94), vol. 3, pp. 1626-1631, Sept., 1994.

[8] C. H. Liu, F. M. Chung, Y. Chen, C. H. Chiu, and T. L. Chen, “Optimal design of a motor-driven three-finger soft robotic gripper”, IEEE/ASME Transactions on Mechatronics, vol. 25, no. 4, pp. 1830-1840, 2020.

[9] G. Marani, S. K. Choi, and J. Yuh, “Underwater autonomous manipulation for intervention missions AUVs”, Ocean Engineering, vol. 36, no. 1, pp. 15-23, 2009.

[10] Y. Li, S. Guo, and Y. Wang, “Design and characteristics evaluation of a novel spherical underwater robot”, Robotics and Autonomous Systems, vol. 94, pp. 61-74, 2017.

[11] J. Shahmoradi, E. Talebi, P. Roghanchi, and M. Hassanalian, “A comprehensive review of applications of drone technology in the mining industry”, Drones, vol. 4, no. 3, 34, 2020.

[12] K. Setty, T. van Niekerk, and R. Stopforth, “Generic gripper for an unmanned aerial vehicle”, Procedia CIRP, vol. 91, pp. 486-488, 2020.

[13] Z. Wang, Y. Torigoe, and S. Hirai, “A prestressed soft gripper: design, modeling, fabrication, and tests for food handling”, IEEE Robotics and Automation Letters, vol. 2, no. 4, pp. 1909-1916, 2017.

[14] Z. Wang, S. Hirai, S. Kawamura, “Challenges and opportunities in robotic food handling: a review”, Frontiers in Robotics and AI: Soft Robotics, 8:789107, 2022.

[15] H. Hsiao, F. Wu, J. Sun, J. Zhao, “A novel passive mechanism for flying robots to perch onto surface”, 2022 IEEE International Conference on Robotics and Automation (ICRA), pp. 1183-1189, May, 2022.

[16] Q. Qi, C. Xiang, V. A. Ho, J. Rossiter, “A sea-anemone-inspired, multifunctional, bistable gripper”, Soft Robotics, vol. 9, no. 6, pp. 1040-1051, 2022.

[17] A. Seibel, M. Yildiz, B. Zorlubas, “A gecko-inspired soft passive gripper”, Biomimetics, vol. 5, no. 2, 12, 2020.

[18] K. Nagaoka, H. Minote, K. Maruya, Y. Shirai, K. Yoshida, T. Hakamada, H. Sawada, T. Kubota, “Passive spine gripper for free-climbing robot in extreme terrain”, IEEE Robotics and Automation Letters, vol. 3, no. 3, pp. 1765-1770, 2018.

[19] X. Guo, W. Li, Q. Gao, H. Yan, Y. Fei, W. Zhang, “Self-locking mechanism for variable stiffness rigid-soft gripper”, Smart Materials and Structures, 29:0.5033, 2020.

[20] Y. Li, Y. Chen, Y. Yang, Y. Wei, “Passive particle jamming and its stiffening of soft robotic grippers”, IEEE Transactions on Robotics, vol. 33, no. 2, pp. 446-455, 2017.

[21] J. Hsu, E. Yoshida, K. Harada, A. Kheddar, “Self-locking underactuated mechanism for robotic gripper”, 2017 IEEE International Conference on Advanced Intelligent Mechatronics (AIM), pp. 620-627, Munich, July 2017.

[22] B. Pérez, H. Nykvist, A. F. Brøgger, M. B. Larsen, and M. F. Falkeborg, “Impact of macronutrients printability and 3D-printer parameters on 3D-food printing: A review”, Food chemistry, vol. 287, pp. 249-257, 2019.

[23] Z. Wang, H. Furuta, S. Hirai, and S. Kawamura, “A scooping-binding robotic gripper for handling various food products”, Frontiers in Robotics and AI, 8, 640805, 2021.

[24] S. Makita, and Y. Maeda, “3D multifingered caging: Basic formulation and planning”, IEEE/RSJ International Conference on Intelligent Robots and Systems, pp. 2697-2702, Sept., 2008.

[25] M. Vahedi and A. F. Stappen, “Caging polygons with two and three fingers”, The International Journal of Robotics Research, vol. 27, no. 11-12, pp. 1308-1324, 2008.